

Electronic Supplementary Information (ESI) for Inorganic Chemistry Frontiers

Boosting CO₂ electroreduction to CO with abundant nickel single atom active sites

Wei-juan Wang^a, Changsheng Cao^b, Kaiwen Wang^{c*} and Tianhua Zhou^b

^a College of Chemistry, Fuzhou University, Fuzhou, Fujian 350108, P. R. China.

^b State Key Laboratory of Structural Chemistry, Fujian Institute of Research on the Structure of Matter, Chinese Academy of Sciences (CAS), Fuzhou 350002, China.

^c Beijing Key Lab of Microstructure and Properties of Advanced Materials, Beijing University of Technology, Beijing 100124, P. R. China.

*Corresponding authors at:

Beijing Key Lab of Microstructure and Properties of Advanced Materials

Beijing University of Technology, Beijing 100124, P. R. China

Tel: +86 18811419320

E-mail address: 56wkw@emails.bjut.edu.cn

Contents

Figure S1. SEM images of Ni-TIPA.

Figure S2. (a) TEM image of Ni-SAs-NC. (b, c) Magnified HAAD-STEM images of Ni-SAs-NC.

Figure S3. (a-c) TEM images of Ni-NPs-NC. (d) STEM image of Ni-NPs-NC. (e, f) TEM images of NC.

Figure S4. Raman spectra of Ni-SAs-NC, NC and Ni-NPs-NC.

Figure S5. (a) Nitrogen adsorption-desorption isotherms for Ni-SAs-NC, NC and Ni-NPs-NC. (b) CO₂ adsorption-desorption isotherms of Ni-SAs-NC, NC and Ni-NPs-NC at 298K.

Figure S6. (a) XPS survey spectra of Ni-SAs-NC and Ni-NPs-NC. (b) N 1s XPS spectra of Ni-NPs-NC and Ni-SAs-NC.

Figure S7. CV curves with different scan rates for (a) Ni-SAs-NC, (b) Ni-NPs-NC, (c) NC and (d) Capacitive Δj ($= j_a - j_c$) against scan rates.

Figure S8. (a, b) Magnified HAAD-STEM images of Ni-SAs-NC after 30-hour electrocatalysis.

Table S1. The content of different-type N in Ni-SAs-NC and Ni-NPs-NC.

Table S2. EXAFS data fitting results of Ni-SAs-NC for Ni K edge.

Table S3. Comparisons the CO₂RR performance of Ni-SAs-NC with reported Ni-based SACs.

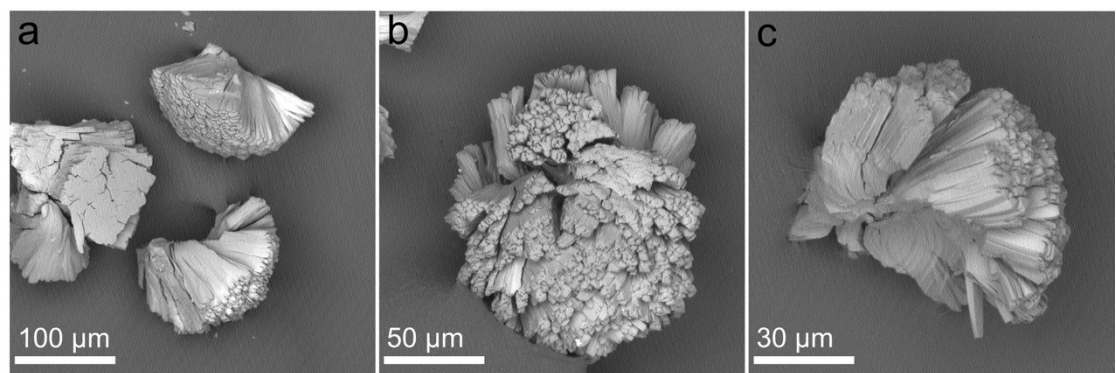


Figure S1. SEM images of Ni-TIPA.

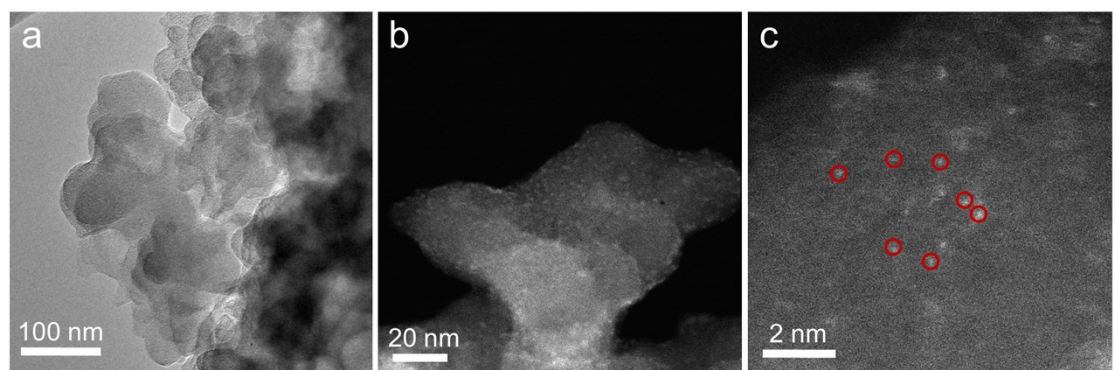


Figure S2. (a) TEM image of Ni-SAs-NC. (b, c) Magnified HAAD-STEM images of Ni-SAs-NC.

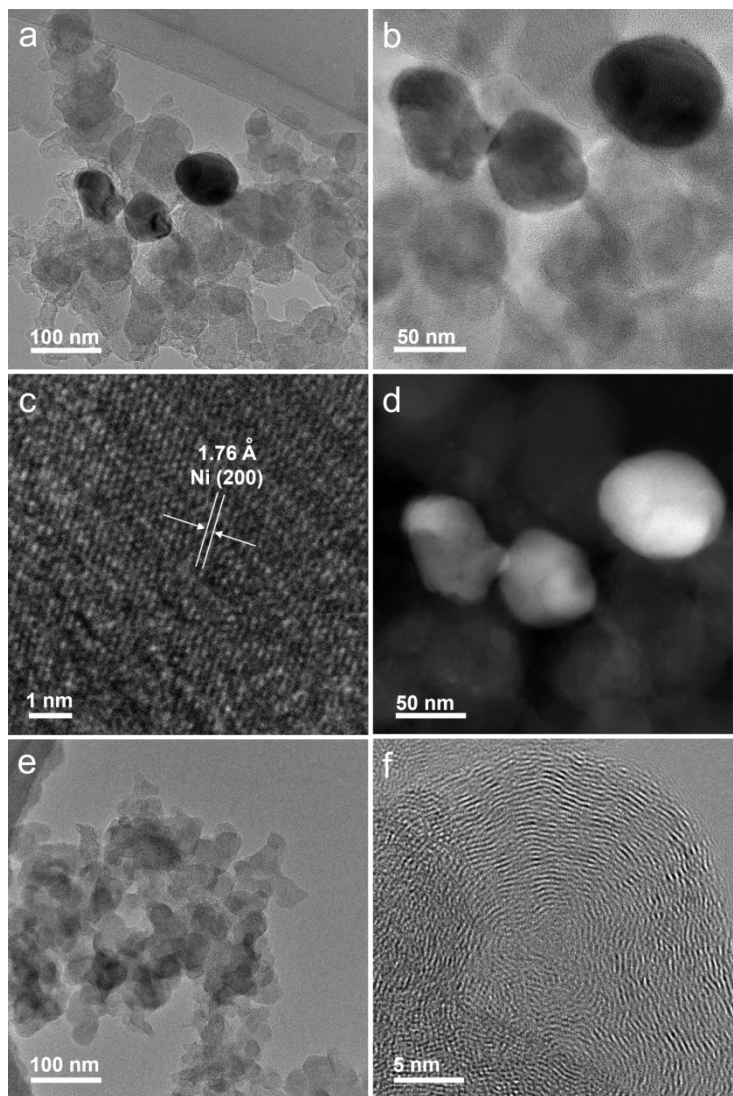


Figure S3. (a-c) TEM images of Ni-NPs-NC. (d) STEM image of Ni-NPs-NC. (e, f) TEM images of NC.

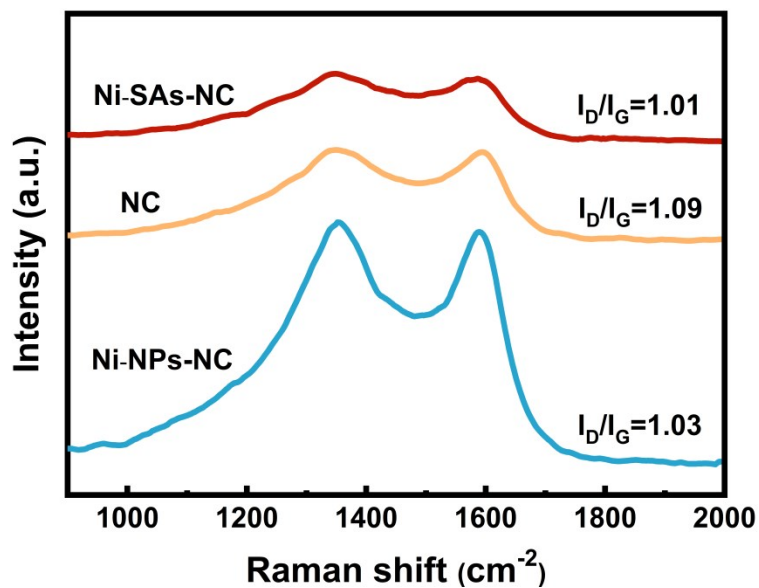


Figure S4. Raman spectra of Ni-SAs-NC, NC and Ni-NPs-NC.

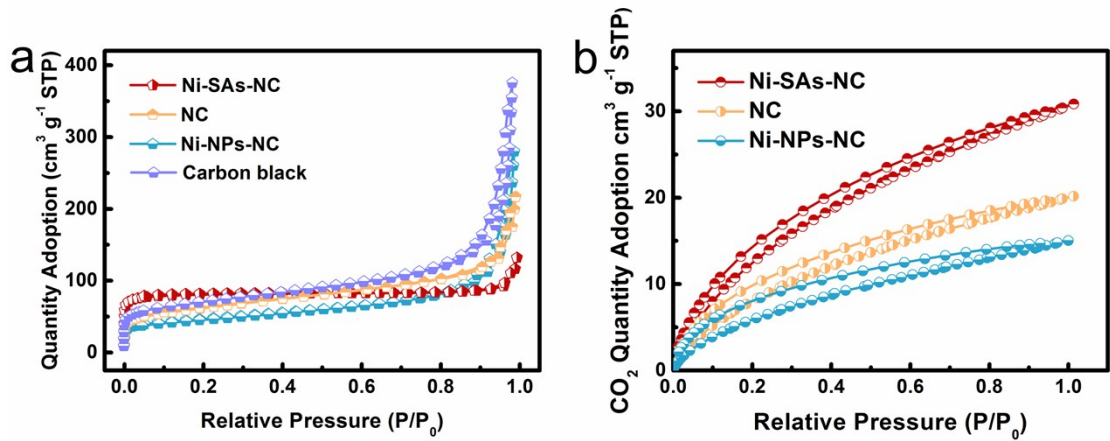


Figure S5. (a) Nitrogen adsorption-desorption isotherms for Ni-SAs-NC, NC, Ni-NPs-NC and carbon black. (b) CO_2 adsorption-desorption isotherms of Ni-SAs-NC, NC and Ni-NPs-NC at 298K.

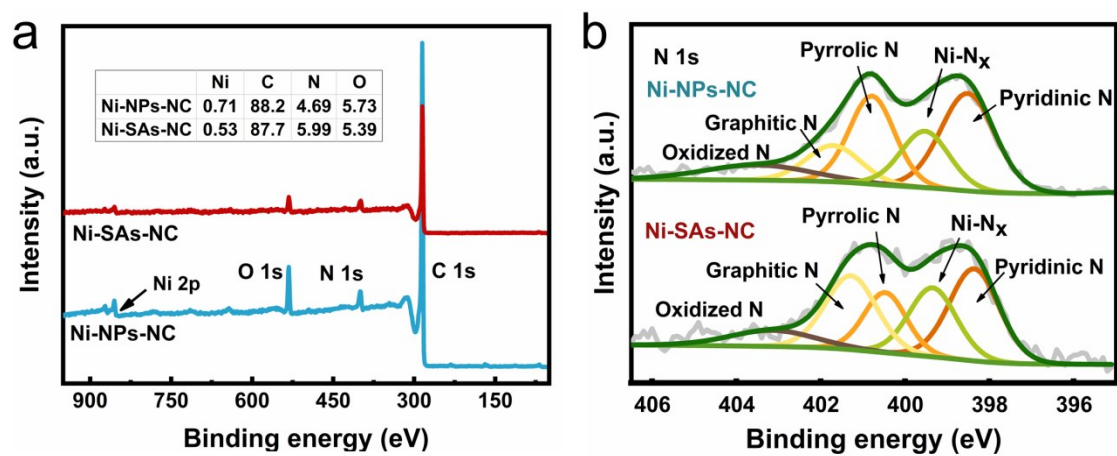


Figure S6. (a) XPS survey spectra of Ni-SAs-NC and Ni-NPs-NC. (b) N 1s XPS spectra of Ni-NPs-NC and Ni-SAs-NC.

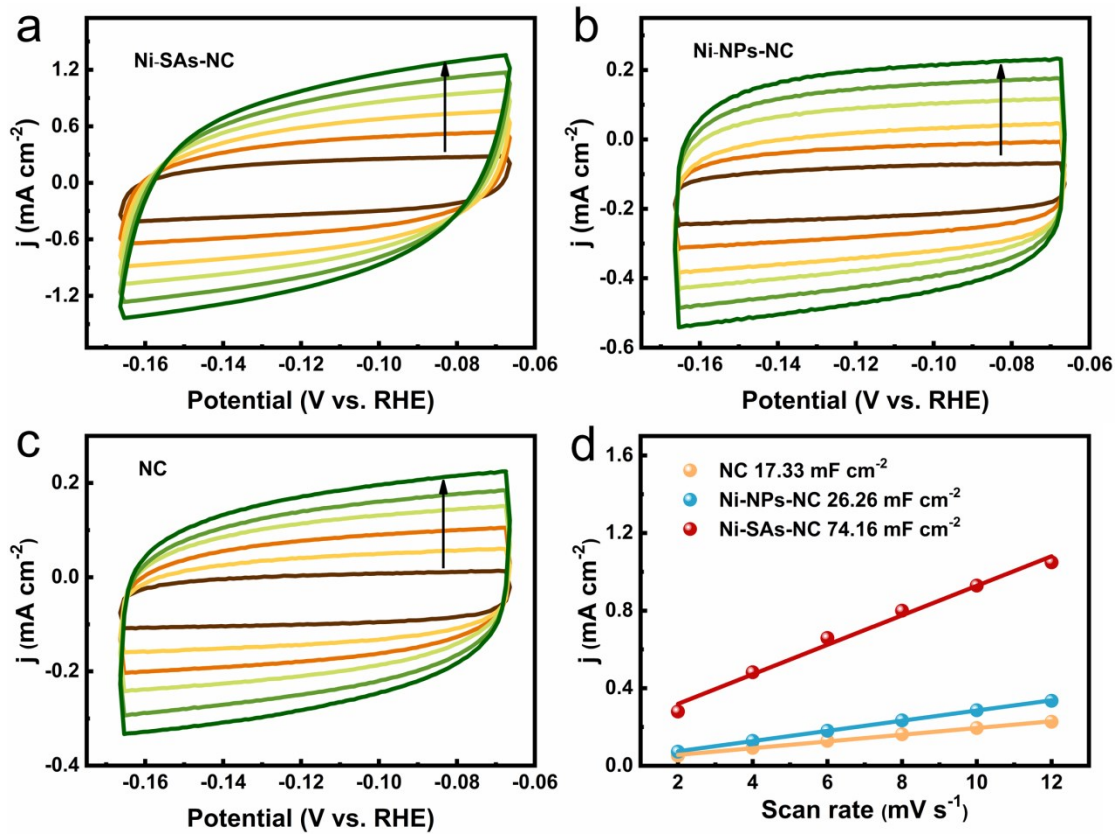


Figure S7. CV curves with different scan rates for (a) Ni-SAs-NC, (b) Ni-NPs-NC, (c) NC and (d) Capacitive Δj ($= j_a - j_c$) against scan rates.

The electrochemically active surface area (ECSA) of the catalysts can be evaluated from the measurements of electrochemical double layer capacitance (C_{dl}), since ECSA can be calculated from the formula of $\text{ECSA} = C_{dl}/C_s$, where C_{dl} corresponds to the slope of the double-layer current versus the scan rates, C_s represents a specific capacitance value ($20 \mu\text{F cm}^{-2}$).^[1] Therefore, the electrochemically active surface area of Ni-SAs-NC, Ni-NPs-NC and NC can be calculated of 3708 cm^2 , 1313 cm^2 , 866.5 cm^2 , respectively.

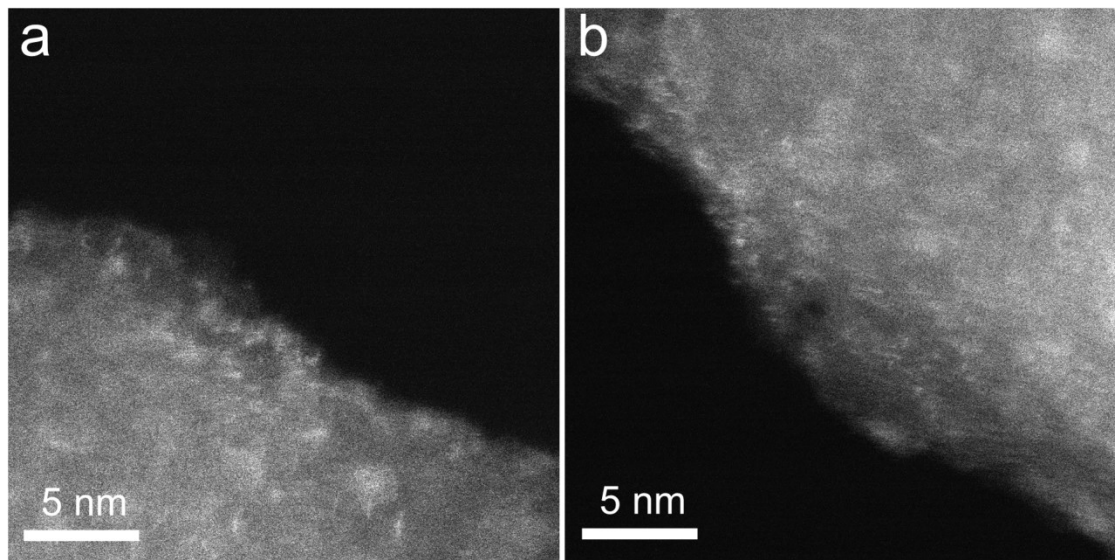


Figure S8. (a, b) Magnified HAAD-STEM images of Ni-SAs-NC after 30-hour electrocatalysis.

Table S1. The content of different-type N in Ni-SAs-NC and Ni-NPs-NC.

	Pyridinic N(%)	Ni-N _x (%)	Pyrrolic N(%)	Graphitic N(%)	Oxidized N(%)
Ni-SAs-NC	25.7	22.4	15.2	27.9	8.8
Ni-NPs-NC	33.9	12.6	25.6	17.6	10.3

Table S2. EXAFS data fitting results of Ni-SAs-NC for Ni K edge.

Sample	Scattering pair	CN	R (Å)	$\sigma^2(10^{-3}\text{\AA}^2)$	ΔE_0 (eV)	R factor
Ni-T@CB	Ni-N	4.0	1.97	0.00872	-4.542	0.028

Table S3. Comparisons the CO₂RR performance of Ni-SAs-NC with reported Ni-based SACs.

Catalyst	Ni content	FE _{CO} (%)	j (mA/cm ²)	Overpotential (mV)	Reference
Ni-SAs-NC	2.0 wt%	98	32	540	This work
C-Zn1Ni4	5.44 wt%	92	70	420	<i>Energy Environ. Sci.</i> , 2018 , <i>11</i> , 1204-1210
Ni-N-C	1.25 wt%	91.2	15	790	<i>Catal. Sci. Technol.</i> , 2019 , <i>9</i> , 3669
Ni-C-Gr	2.2 wt%	95	3	590	<i>Small</i> , 2016 , <i>12</i> , 6083-6089
Ni-CNT-CC	0.27 wt%	95	95	540	<i>Angew. Chem., Int. Ed.</i> , 2020 , <i>59</i> , 798-803
Ni _{SA} -N ₂ -C	0.9 wt%	98	26	690	<i>Angew. Chem., Int. Ed.</i> , 2020 , <i>59</i> , 2705-2709
NiN-GS	2 at%	95	24	550	<i>Chem</i> , 2017 , <i>3</i> , 950-960
A-Ni-NSG	2.8 wt%	97	95	500	<i>Nat. Energy</i> , 2018 , <i>3</i> , 140-147
NiSA/PCFM	1.3 wt%	96	30	590	<i>Nat. Commun.</i> , 2020 , <i>11</i> , 593
Ni-Fe-N-C	0.97 wt%	98	20	590	<i>Angew. Chem., Int. Ed.</i> , 2019 , <i>58</i> , 6972-6976
Ni-NCB	0.27 wt%	99	22	571	<i>Joule</i> , 2019 , <i>3</i> , 265-278
Ni-SAC	1.8 wt%	98.9	4	1090	<i>Nat. Commun.</i> , 2019 , <i>1</i> , 4585

Reference

1. H. B. Yang, S.-F. Hung, S. Liu, K. Yuan, S. Miao, L. Zhang, X. Huang, H.-Y. Wang, W. Cai, R. Chen, J. Gao, X. Yang, W. Chen, Y. Huang, H. M. Chen, C. M. Li, T. Zhang and B. Liu, *Nat. Energy*, 2018, **3**, 140-147.